

Preparation and properties of ferroelectric $\text{Pb}_{1-x}\text{Ca}_x\text{TiO}_3$ thin films produced by the polymeric precursor method

D. S. L. PONTES, E. R. LEITE, F. M. PONTES, E. LONGO
*Department of Chemistry, Federal University of São Carlos-UFSCar,
 Caixa Postal 676, 13560-905 São Carlos, SP, Brazil*

J. A. VARELA
Institute of Chemistry, UNESP, Caixa Postal 355, 14801-970 Araraquara, SP, Brazil

$\text{Pb}_{1-x}\text{Ca}_x\text{TiO}_3$ thin films with $x = 0.24$ composition were prepared by the polymeric precursor method on Pt/Ti/SiO₂/Si substrates. The surface morphology and crystal structure, and the ferroelectric and dielectric properties of the films were investigated. X-ray diffraction patterns of the films revealed their polycrystalline nature. Scanning electron microscopy (SEM) and atomic force microscopy (AFM) analyses showed the surface of these thin films to be smooth, dense and crack-free with low surface roughness. The multilayer $\text{Pb}_{1-x}\text{Ca}_x\text{TiO}_3$ thin films were granular in structure with a grain size of approximately 60–70 nm. The dielectric constant and dissipation factor were, respectively, 174 and 0.04 at a 1 kHz frequency. The 600-nm thick film showed a current density leakage in the order of 10^{-7} A/cm² in an electric field of about 51 kV/cm. The C-V characteristics of perovskite thin films showed normal ferroelectric behavior. The remanent polarization and coercive field for the deposited films were 15 $\mu\text{C}/\text{cm}^2$ and 150 kV/cm, respectively.

© 2001 Kluwer Academic Publishers

1. Introduction

Ferroelectric thin films have been extensively studied for possible use in nonvolatile memories [1, 2], pyroelectric detectors [3], and optical wave-guides [4]. Among the various ferroelectrics, PZT thin films have been intensively investigated [5, 6], while PbTiO_3 thin films have received little attention. Owing to their good ferroelectric properties, however, calcium-modified lead titanate ($\text{Pb}_{1-x}\text{Ca}_x\text{TiO}_3$) thin films are promising candidates for non-volatile memories. Yamaka *et al.* [7] reported highly *c*-axis oriented (Pb, Ca)TiO₃ thin films on MgO and SrTiO₃ substrates by the r.f. magnetron sputtering technique. Other authors have also reported on the production of (Pb, Ca)TiO₃ thin films, among them Maiwa *et al.* [8], who reported on the preparation of $\text{Pb}_{0.7}\text{Ca}_{0.3}\text{TiO}_3$ thin films by a multiple-cathode r.f. magnetron sputtering method. In addition, Bao *et al.* [9] prepared (Pb, Ca)TiO₃ thin films by a modified sol-gel technique, and other authors have also discussed the influence of calcium on the ferroelectricity of modified lead titanate on the form of the bulk [10, 11]. Although the substitution of Pb by Ca produces a reduction of the Curie temperature, which implies a lower coercive field at room temperature, the preparation of ($\text{Pb}_{1-x}\text{Ca}_x\text{TiO}_3$) thin films by the polymeric precursor method (Pechini's method) [12–16] has yet not been reported. The main advantages of this method are the easy production of

homogeneous stoichiometric ceramic thin films, which are usually polycrystalline at relatively low temperatures and the use of inexpensive deposition techniques such as spin- or dip-coating.

This paper describes the synthesis and properties of $\text{Pb}_{1-x}\text{Ca}_x\text{TiO}_3$ thin film prepared by the Pechini process.

2. Experimental procedure

$\text{Pb}_{1-x}\text{Ca}_x\text{TiO}_3$ thin films with nominal $\text{Pb}_{0.76}\text{Ca}_{0.24}\text{TiO}_3$ compositions were synthesized. In this synthesis, metal cations are chelated in a solution using hydroxycarboxylic acid as the chelating agent. The solution is mixed with a polyhydroxyalcohol and heated to promote esterification reactions in the solution. The metals remain homogeneously distributed in the polymeric network. A flow chart of the $\text{Pb}_{0.76}\text{Ca}_{0.24}\text{TiO}_3$ synthesis used in this study is given in Fig. 1.

Lead (II) acetate trihydrate ($\text{Pb}(\text{CH}_3\text{COO})_2 \cdot 3\text{H}_2\text{O}$), calcium carbonate (CaCO_3) and titanium (IV) isopropoxide ($\text{Ti}(\text{OCH}(\text{CH}_3)_2)_4$) were used as starting materials. Ethylene glycol and citric acid were used as polymerization/complexation agents for the process. Ammonium hydroxide was used to adjust the pH and to prevent lead citrate precipitation. The molar ratio among the Lead-calcium and titanium cations was 1:1,

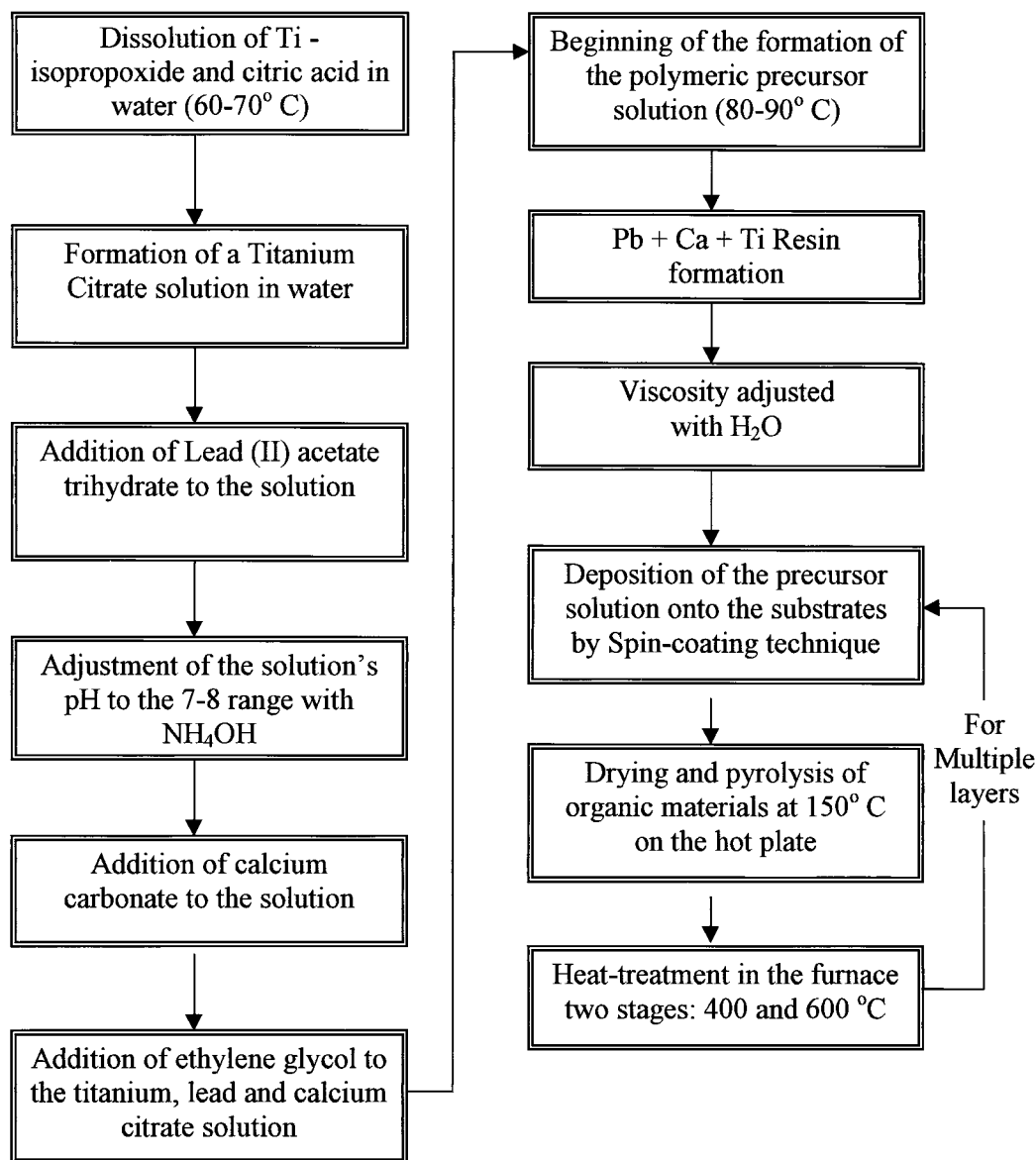


Figure 1 Flow-chart illustrating the procedure for the preparation of $(\text{Pb}_{0.76}\text{Ca}_{0.26})\text{TiO}_3$ solution and film production.

the citric acid/metal molar ratio was fixed at 1.00, and the citric acid/ethylene glycol ratio was fixed at 60/40 (mass ratio). The viscosity of the deposition solution was adjusted to 25 mPa.s by controlling the water content. Pt(111)/Ti/SiO₂/Si(100) wafers were used as substrates. The substrate was spin-coated by dropping a small amount of the polymeric precursor solution onto it. Rotation speed and spin time were set at 4000 rpm and 30 s, respectively. After deposition, each layer was dried at 150°C on a hot plate for 20 min to remove residual solvents. The heat treatment was carried out in two stages: initial heating at 400°C for 2 h at a heating rate of 5°C/min to pyrolyze the organic materials, followed soon thereafter by heating to crystallize them. Each layer was pyrolyzed at 400°C and crystallized before the next layer was coated. This process was repeated several times to achieve the desired film thickness.

X-ray diffraction (XRD) patterns were obtained using a Cu K_α radiation source to determine the phase of the films. The thickness of the coated film was measured by thin film cross-section analysis using scanning

electron microscopy (SEM). Atomic force microscopy (AFM) was used to obtain a 3D-image reconstruction of the sample surface. These images allow for an accurate analysis of the sample surface and the quantification of very important parameters such as roughness and grain size. A Digital Instruments Multi-Mode Nanoscope IIIa was used.

The ferroelectric properties of the $\text{Pb}_{0.76}\text{Ca}_{0.24}\text{TiO}_3$ thin film were evaluated using a capacitor structure of metal-ferroelectric-metal, onto which the Au (0.3-mm diameter) top electrode was deposited by sputtering through a designed mask onto the film surfaces. Ferroelectric properties was performed using the Radiant Technologies RT6000HVS ferroelectric testing system. The capacitance-voltage (C-V) properties were characterized using a Hewlett-Packard (4194A) impedance/gain phase analyzer, in which the capacitance value was measured by a small AC signal of 10 mV at 100 kHz. The dielectric constant and dissipation factor were measured as a function of frequency in the range of 100 Hz to 10 MHz. The leakage current-voltage (I-V) characteristic was measured with

a voltage source measuring unit (Keithley 237). All the measurements were done at room temperature.

3. Results and discussions

The X-ray diffraction (XRD) pattern of $\text{Pb}_{0.76}\text{Ca}_{0.24}\text{TiO}_3$ thin film on a $\text{Pt}(111)/\text{Ti}/\text{SiO}_2/\text{Si}(100)$ substrate is displayed in Fig. 2. The XRD analysis revealed that a $\text{Pb}_{0.76}\text{Ca}_{0.24}\text{TiO}_3$ thin film with a perovskite structure was formed by annealing at 600°C for 2 hours. The diffractogram shows sharp well-defined diffrac-

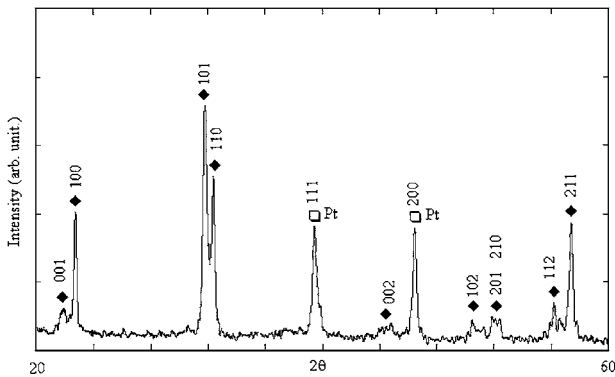


Figure 2 XRD patterns of the $\text{Pb}_{0.76}\text{Ca}_{0.24}\text{TiO}_3$ thin film at 600°C .

tion peaks, indicating a high degree of crystallinity. The (001/100) and (101/110) peaks appearing on the diffractogram indicate that the film is tetragonally structured, which is confirmed by the ferroelectric behavior of these films described later herein. The tetragonal crystallographic parameters thus obtained showed an acceptable tetragonal distortion of $c/a \sim 1.037$. Analogous XRD patterns have been observed by other authors [17, 18].

Fig. 3 shows typical SEM micrograph of multilayer $\text{Pb}_{0.76}\text{Ca}_{0.24}\text{TiO}_3$ thin film prepared on $\text{Pt}/\text{Ti}/\text{SiO}_2/\text{Si}$ substrates at 600°C , in which the interface between the PCT layer and substrate can be very clearly seen. This figure shows a thin film with a 600-nm-thick multilayer structure.

AFM imaging was carried out in the contact mode using a triangular shaped 200-micron long cantilever with a spring constant of 0.06 N/m. The scanning rate was varied from 1 to 2 Hz and the applied force from 10 to 50 nN, depending on the sample/tip interactions. The surface roughness (rms) was calculated using the equipment's software routine. The grain size of the film heat treated at 600°C was estimated to be approximately 60–70 nm and the surface roughness is 2.7 nm (Fig. 4a). The film surface appeared to be densely packed, smooth and free of cracks or voids (Fig. 4b). Sirera *et al.* [18]

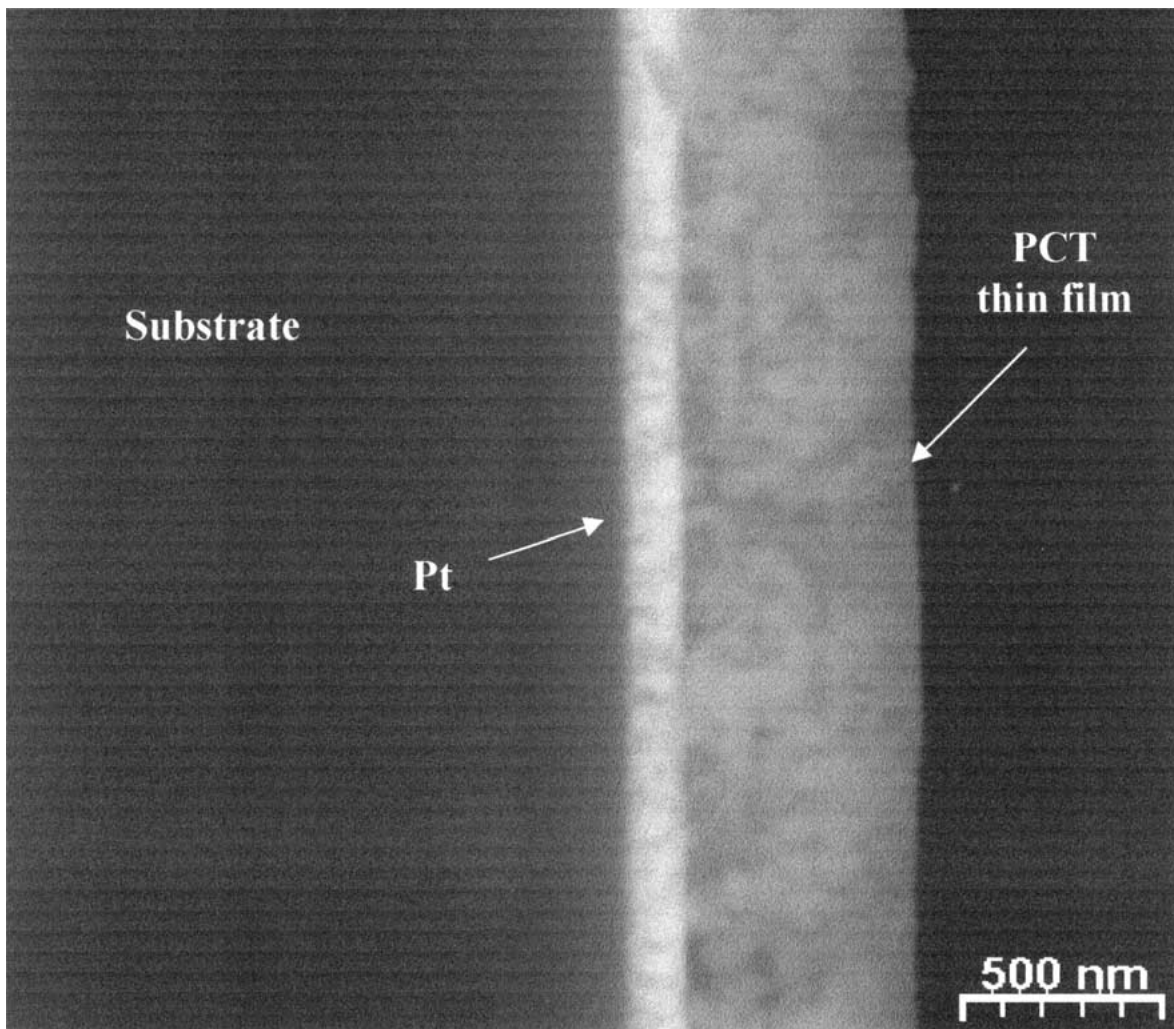


Figure 3 Cross-section microstructure of PCT thin films heat-treated at 600°C .

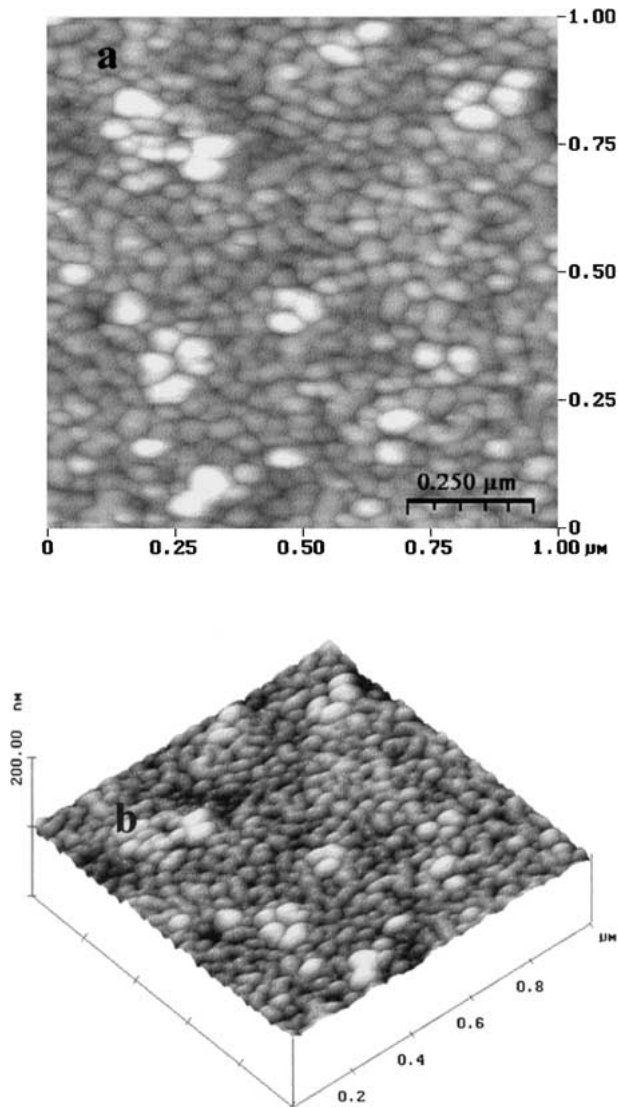


Figure 4 Atomic force micrograph of PCT film (a) 2D-image and (b) 3D-image, on the Si/SiO₂/Ti/Pt substrate at 600°C.

produced a microstructure of PCT thin films obtained by sol-gel processing with grains of about 50–100 nm, which was associated to the presence of 600 nm clusters and, thus, had an inhomogeneous appearance.

A 600-nm thick film was used for the electrical and ferroelectric measurements. Fig. 5 illustrates the variation of the dielectric constant and the dissipation factor ($\tan \delta$) as a function of frequency, in the range of 100 Hz to 10 MHz, for the films deposited on Pt/Ti/SiO₂/Si substrates. The dielectric properties of different dot electrodes on the films changed by 2–3%, indicating the homogeneous composition and uniform thickness of the PCT thin films prepared by the polymeric precursor method. The dielectric constant and the dissipation factor ($\tan \delta$) at a 1 kHz frequency were 174 and 0.04, respectively. This film, which showed little dielectric constant dispersion, displayed a decline of approximately 18% when the applied frequency is increased from 100 Hz to 10 MHz. On the other hand, the rapid increase of the dissipation factor at a frequency above 10⁶ Hz may have been caused by a contact resistance between the probe and the electrode. In addition, Bao *et al.* [9] reported PCT thin film in which the dielec-

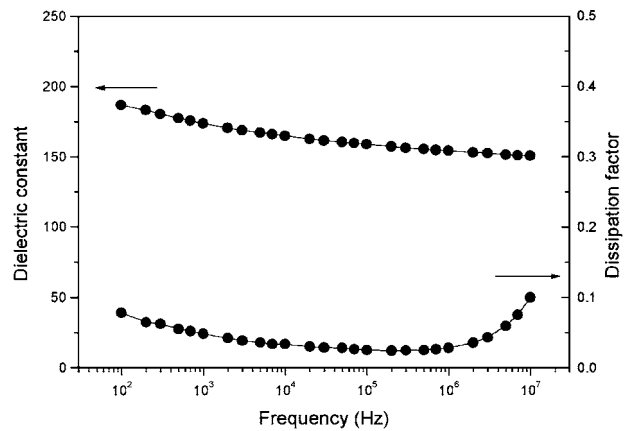


Figure 5 Dielectric constant and dissipation factor of PCT film as a function of frequency.

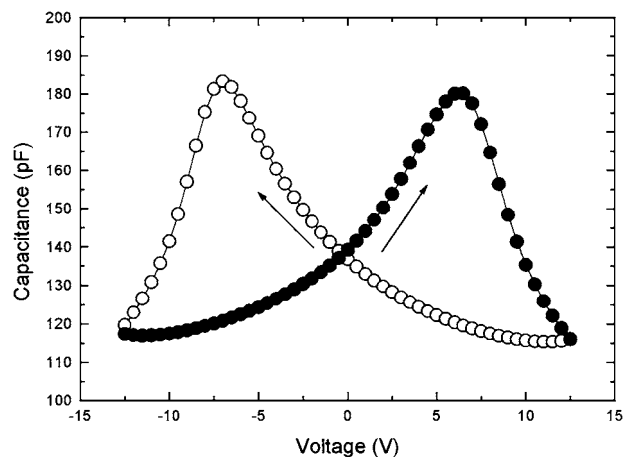


Figure 6 C-V characteristics of the PCT thin film.

tric constant and dissipation factor measurements as a function of frequencies in the range of 1 kHz to 1 MHz showed a decline greater than 55% above 10³ kHz. Calzada *et al.* [20] reported a dielectric constant value of 116 for a sol-gel derived modified PCT thin film with the same composition, prepared by rapid heating heat-treatment and a dielectric constant value of 42 obtained by the conventional heat-treatment. Other authors [21] have reported PCT thin films with a dielectric constant value of 171 for 1000-nm thick films with an $x = 0.3$ composition.

Fig. 6 illustrates the typical C-V curve for MFM capacitors. Capacitance dependence on the voltage is strongly nonlinear, which confirms the ferroelectric properties of the film resulting from ferroelectric domain switching. The C-V curve also displays symmetry in the maximum capacitance values that can be observed in the vicinity of the spontaneous polarization switching. The C-V curve is symmetric around the zero bias axis, indicating that the films contain few movable ions or charge accumulation at the film/electrode interface. On the other hand, the center of the C-V curves were not located in the zero bias field for PCT thin films (same composition) obtained by a modified sol-gel technique, but shifted toward the positive bias field [9]. The ferroelectric properties of the PCT film were confirmed by hysteresis measurements.

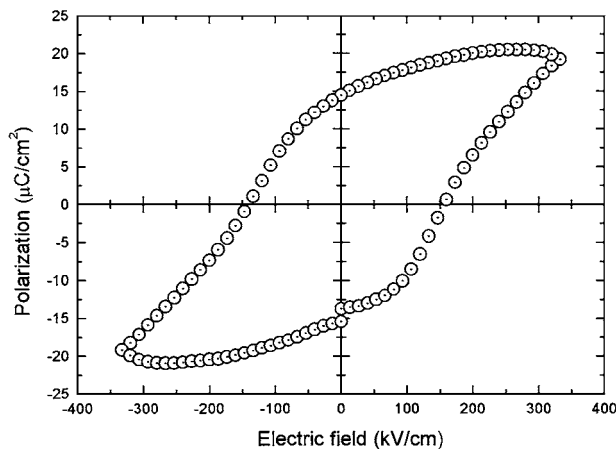


Figure 7 Hysteresis loop of a $\text{Pb}_{0.76}\text{Ca}_{0.24}\text{TiO}_3$ thin film.

Fig. 7 shows a typical hysteretic loop of a thin film annealed at 600°C . Ferroelectricity was clearly confirmed by the highest remanent polarization measured in this study. Fig. 6 identifies the remanent polarization $P_r = 15 \mu\text{C}/\text{cm}^2$ and coercive field $E_c = 150 \text{ kV}/\text{cm}$, respectively. Other researchers have reported PCT thin film obtained by the sol-gel [20] technique with remanent polarization (P_r) of $\sim 6 \mu\text{C}/\text{cm}^2$ and a coercive field in the order of $100 \text{ kV}/\text{cm}$. Martín *et al.* [22] have reported PCT thin films with an $x = 0.24$ composition obtained by pulsed-laser deposition, with remanent polarization (P_r) of $\sim 0.55 \mu\text{C}/\text{cm}^2$ and a coercive field in the order of $200 \text{ kV}/\text{cm}$. Tsuzuki *et al.* [21] also reported PCT thin films with an $x = 0.3$ composition obtained by the sol-gel method with remanent polarization (P_r) of $\sim 4.1 \mu\text{C}/\text{cm}^2$ and a coercive field in the order of $68 \text{ kV}/\text{cm}$.

Fig. 8 shows the current-voltage characteristics of the MFM capacitor structure with a 600-nm thick PCT film, which was measured with a voltage step of 0.1 V and a time lapse of 1.0 s . In the $\log J$ versus $\log V$ plot, the leakage current density increases linearly with the external electric field in the region of the low electric field, with a 1.0 slope, indicating an ohmic-like conduction mechanism. Above the critical field, the leakage current density increases non-linearly because con-

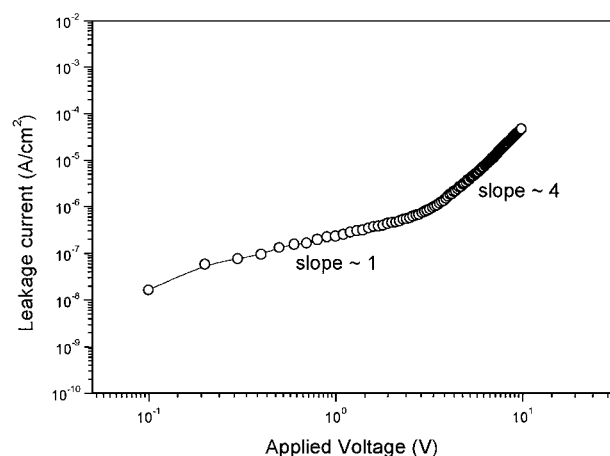


Figure 8 Logarithm of current density $\log(J)$ is plotted as function of the logarithm of applied voltage $\log(V)$. Two regions of different slopes can be observed.

duction of the current is governed by another emission mechanism (either Schottky or Pool-Frenkel). In the high field region, the $\log(J)$ vs. $\log(V)$ curve shows a slope of >4 . The leakage current level of the PCT thin film obtained by the polymeric precursor method was in the order of $10^{-7} \text{ A}/\text{cm}^2$ of approximately 3 V ($51 \text{ kV}/\text{cm}$). This value is of the same order of magnitude as the typical values of PCT films grown by the multiple-cathode sputtering method reported by Maiwa and Ichinose [8].

4. Conclusions

Ferroelectric lead calcium titanate [$(\text{Pb}_{0.76}\text{Ca}_{0.24})\text{TiO}_3$] thin films deposited on platinum-coated silicon substrates by the spin-coating process were successfully produced using the polymeric precursor method. Polycrystalline PCT thin films having a tetragonal perovskite structure were obtained. Dense, homogeneous, crack-free, smooth and uniformly thick PCT thin films were produced by spin-coating and thermal annealing in a conventional furnace at 600°C . The ferroelectric nature of the PCT films was confirmed by the existence of P-E hysteresis curves and by butterfly-shaped C-V curves. The ferroelectric properties were $P_r = 15 \mu\text{C}/\text{cm}^2$ and $E_c = 150 \text{ kV}/\text{cm}$. The dielectric constant and dissipation factor were, respectively, 174 and 0.04 at a 1 kHz frequency. The 600-nm thick film showed a current density leakage in the order of $10^{-7} \text{ A}/\text{cm}^2$ in an electric field of approximately $51 \text{ kV}/\text{cm}$. The results of this investigation allow us to conclude that PCT thin films produced by the polymeric precursor method are promising candidates for application in a variety of devices.

Acknowledgments

The authors gratefully acknowledge the financial support of the Brazilian research funding agencies FAPESP, CNPq, PRONEX and CAPES.

References

1. H. KUMAZAWA and K. MASUDA, *Thin Solid Films* **353** (1999) 144.
2. C. R. CHO, L. F. FRANCIS and D. L. POLLA, *Mater. Lett.* **38** (1999) 125.
3. T. IMAI, M. MAEDA and I. SUZUKI, *J. Korean Phys. Soc.* **32** (1998) S1485.
4. C. LEE, V. SPIRIN, H. SONG and K. NO, *Thin Solid Films* **340** (1999) 242.
5. S.-H. KIM, Y.-S. CHOI, C.-E. KIM and D.-Y. YANG, *ibid.* **325** (1998) 72.
6. H. M. CHEN and J. Y. M. LEE, *Appl. Phys. Lett.* **73** (1998) 309.
7. E. YAMAKA, H. WATANABE, H. KIMURA, H. KANAYA and H. OHKUMA, *J. Vac. Sci. Technol. A* **6**(5) 1988) 2921.
8. H. MAIWA and N. ICHINOSE, *Jpn. J. Appl. Phys.* **36**(9b) (1997) 5825.
9. D. BAO, X. WU, L. ZHANG and X. YAO, *Thin Solid Films* **350** (1999) 30.
10. J. MENDIOLA, C. ALEMANY, L. PARDO and A. GONZALEZ, *Ferroelectrics* **94** (1989) 209.
11. J. MENDIOLA, B. JIMÉNEZ, C. ALEMANY, L. PARDO and L. DEL OLMO, *Ferroelectrics* **94** (1989) 183.

12. F. M. PONTES, E. R. LEITE, E. LONGO, J. A. VARELA, E. B. ARAUJO and J. A. EIRAS, *Appl. Phys. Lett.* **76**(17) (2000) 2433.
13. F. M. PONTES, E. B. ARAUJO, E. R. LEITE, J. A. EIRAS, E. LONGO, J. A. VARELA and M. A. PEREIRA-DA-SILVA, *J. Mater. Res.* **15**(5) (2000).
14. F. M. PONTES, J. H. G. RANGEL, E. R. LEITE, E. LONGO, J. A. VARELA, E. B. ARAUJO and J. A. EIRAS, *Thin Solid Films* **366**(1-2) (2000) 232.
15. F. M. PONTES, E. L. LONGO, J. H. RANGEL, M. I. BERNARDI, E. R. LEITE and J. A. VARELA, *Mater. Lett.* **43** (2000) 249.
16. S. M. ZANETTI, E. LONGO, J. A. VARELA and E. R. LEITE, *ibid.* **31** (1997) 173.
17. S. CHEWASATN and S. J. MILNE, *J. Mat. Sci.* **32** (19997) 575.
18. R. SIRERA, M. L. CALZADA, F. CARMONA and B. JIMÉNEZ, *J. Mat. Sci. Lett.* **13** (1994) 1804.
19. D. BAO, X. WU, L. ZHANG and X. YAO, *Thin Solid Films* **350** (1999) 30.
20. M. L. CALZADA, J. MENDIOLA, F. CARMONA, P. RAMOS and R. SIRERA, *Mat. Res. Bull.* **31**(4) (1996) 413.
21. A. TSUZUKI, H. MURAKAMI, K. KANI, K. WATARI and Y. TORII, *J. Mat. Sci. Lett.* **10** (1991) 125.
22. M. J. MARTÍN, J. MENDIOLA and C. ZALDO, *J. Am. Ceram. Soc.* **81**(10) (1998) 2542.

*Received 19 May 2000
and accepted 1 February 2001*